Velocity and structural information extracted from shot gathers obtained from ambient noise using seismic interferometry

Deyan Draganov[*,1], *Xander Campman*[2], *Jan Thorbecke*[1], *Arie Verdel*[2], *Kees Wapenaar*[1],
[1] *Department of Geotechnology, Delft University of Technology, Stevinweg 1, 2628CN Delft, The Netherlands*
[2] *Shell International E&P B.V., Kessler Park 1, 2288 GS Rijswijk, The Netherlands*

SUMMARY

Application of seismic interferometry to ambient seismic noise can retrieve the Green's function of the medium including its reflection response. This method has been applied to ambient noise recorded in Libya. The retrieved common-shot gathers and stacked time-migrated sections have been compared to shot gathers and stacked sections from an active survey at the same area to reveal that several reflectors have been retrieved. Here, we show how we processed the retrieved common-shot gathers to extract velocity and structural information of the subsurface. This information was then used to obtain the retrieved stacked time-migrated images.

INTRODUCTION

Ambient seismic noise has always attracted much attention from seismologists. Knowledge of the characteristics of noise measured at installation sites is essential for optimally designing seismic stations and arrays, for example. Aki (1957) was the first to suggest noise can also be used to extract information about the Earth's structure. He developed a method based on spatial autocorrelations to extract surface-wave phase-velocity information from stationary noise. Since the 1990's, this method has been developed further and is now used mainly in geotechnical- and earthquake engineering (Okada, 2003).

Here we attempt to obtain velocity information from reflections extracted from ambient seismic noise. Claerbout (1968) showed that for a 1D acoustic medium the autocorrelation of the observed transmission response yields the reflection response of that medium. Wapenaar et al. (2002) and Wapenaar (2004) proved this concept for 3D inhomogeneous acoustic and elastic media for crosscorrelation of recordings from transient as well as noise sources. Later, this process was termed seismic interferometry (SI). The theory shows that the crosscorrelation process retrieves the complete Green's function, including surface waves and reflections. While the retrieval of surface waves from noise (Campillo and Paul, 2003; Shapiro et al., 2005) is quite robust, retrieval of reflections has proven much more difficult. Using standard seismic-data processing techniques to suppress the undesired surface-wave noise and to bring forward the more subtle body-wave noise, Draganov et al. (2009) retrieved reflection arrivals from approximately 11 hours ambient noise recorded in Libya. In the following, we briefly review these results and then show with examples how the retrieved virtual shot gathers are processed to obtain velocity and structural information of the subsurface.

RETRIEVAL OF REFLECTIONS FROM NOISE

In 2007, Shell carried out a passive seismic experiment in the northeastern part of the Sirte Basin, East of Ajdabeya, Libya. About 11 hours of ambient noise was recorded and stored in about 900 time windows of 47 seconds. The noise was recorded along 8 parallel lines, lying 500 m apart. Around 14 km from the southeast end, the lines were bisected by a traffic road. Each line consists of about 400 receiver stations with 50 m spacing. Each station consists of a group of 48, 10 Hz, vertical-component geophones. Draganov et al. (2009) applied SI by crosscorrelating the recorded ambient noise to obtain virtual common-shot gathers. Figure 1(a) shows a virtual shot gather at 1 km along one of the receiver lines. A comparison of this gather with a shot gather recorded using a seismic vibrator at approximately the same position (Figure 1(b)) shows that several coherent events, highlighted in green, can be interpreted as retrieved reflections. The correlation procedure was repeated

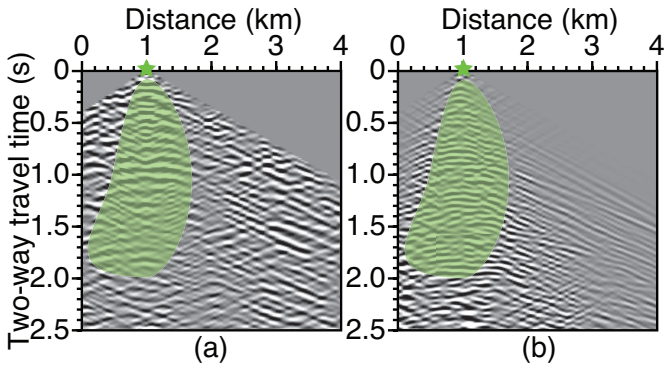

Figure 1: *Comparison between **(a)** a virtual common-shot gather retrieved from the ambient noise using SI and **(b)** a common-shot gather from a vibrator source at the location of the virtual source. The green stars indicate the (virtual) shot positions. The green areas highlight hyperbolic events that coincide in time.*

for each receiver position along the same line thus resulting in the retrieval of 412 virtual common-shot gathers.

PROCESSING OF THE RETRIEVED DATA

The application of SI to ambient subsurface noise should retrieve virtual shot gathers, which in theory are identical, apart from shot-generated and surface noise, to shot gathers that would be recorded with active sources. This means that the retrieved data could be processed just like active data to obtain a stacked section of the subsurface. In the following, we apply some standard processing steps to the retrieved data. This is illustrated with examples for the above-mentioned line.

During the correlations, correlation artefacts may appear in the retrieved shot gathers before the estimated arrival times of the direct wave. To mitigate these unwanted contributions, we mute everything at times earlier than the estimated arrival of

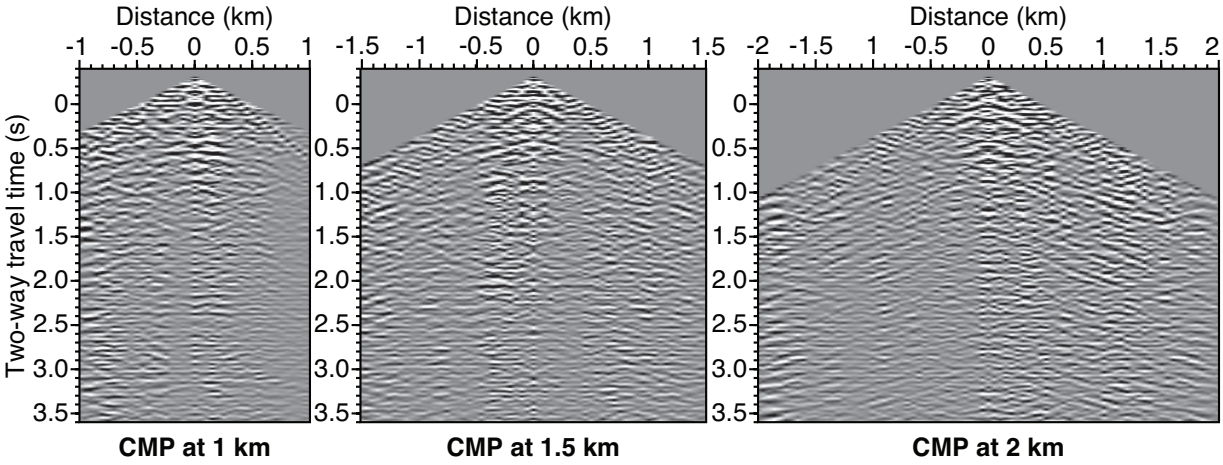

Figure 2: *Common-midpoint (CMP) gathers obtained from the retrieved virtual shot gathers for CMPs situated (from left to right) 1 km, 1.5 km, and 2 km away from the southeast end of the line.*

the direct wave. We then apply near-surface corrections to the virtual shot gathers. As in the active data processing, we use a constant near-surface velocity to redatum the gathers to MSL (mean sea level). In the active data, this is followed by one pass of residual statics. We omitted this step. After statics, we sort the retrieved common-shot gathers into common-midpoint (CMP) gathers. Figure 2 shows three CMP gathers obtained from the virtual shot gathers. At earlier times, up to about 2 s $\sim$ 2.5 s, some distinct hyperbolic arrivals can be identified, which can be used in velocity analysis to estimate stacking velocities. At later times, no reflections can be distinguished, which makes velocity estimation for these later times difficult. The nearer the CMP is located to the 14th kilometer (i.e., the traffic road), the more difficult it is to distinguish reflections. This may be attributed to remnant surface waves, caused by traffic on the road. The geophone patterns were designed to suppress surface waves with the most dominant wave numbers in both inline and crossline direction for the active data. The noise, however, contains significant energy at lower frequencies. Frequency and inline frequency-wavenumber filters were used before crosscorrelation to further suppress the surface waves, but still surface waves propagating at angles different from the inline direction from the road to the survey line are present. Furthermore, there is aliased surface-wave energy. The low signal-to-noise ratio of reflections in Figure 2 makes the velocity picking even more difficult as in a velocity spectrum the maxima are not clearly defined in this case.

After the CMP sorting, we subject the retrieved data to velocity analysis. We make combined use of velocity semblance plots and constant-velocity stacks to pick stacking velocities every 0.5 km. Figure 3 shows a graph with picked stacking velocities for several CMPs along the line. For comparison, we also show the stacking velocities picked from the active data by a professional seismic processer. The picking on the active data was performed every 2 km. In general, the velocities picked from the virtual data are lower than the velocities picked from the active data. One reason might be that the events in the retrieved shot gathers are only coherent for limited (short) offsets. As a consequence, the velocity-semblance panels have a lower resolution, making it more difficult to pick the correct

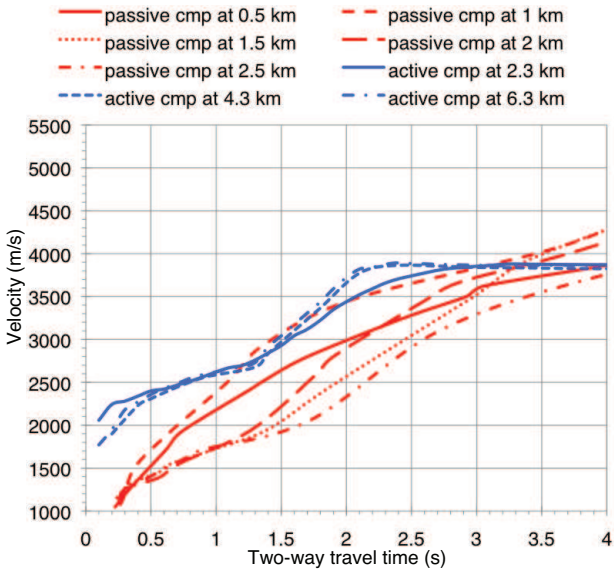

Figure 3: *Stacking velocities picked from the virtual data at CMPs lying at 0.5 km, 1 km, 1.5 km, 2 km, and 2.5 km. For comparison, three stacking-velocity profiles are shown that were picked from the active data at 2.3 km, 4.3, and 6.3 km.*

velocity. Why the velocities from the passive data apear to be consistently lower than from the active data is a current topic of investigation. For a CMP relatively far away from the traffic road (further then 10 km), the stacking velocities from the virtual data for two-way travel times between 1 s and 3.5 s are close to the stacking velocities from the active data. The closer a CMP to the road, the bigger the deviation of the ambient-noise velocities from the active-data velocities. Note that for the CMP at 0.5 km, the fold was not sufficient to perform a better velocity picking.

With the stacking velocities picked, we apply normal-moveout corrections, stacking and phase-shift time migration (see Figure 4(a)) to the virtual data. Figure 4(b) shows the time-migrated stacked section obtained from the active data, which is band-pass filtered to attempt to match the frequency content of (a).

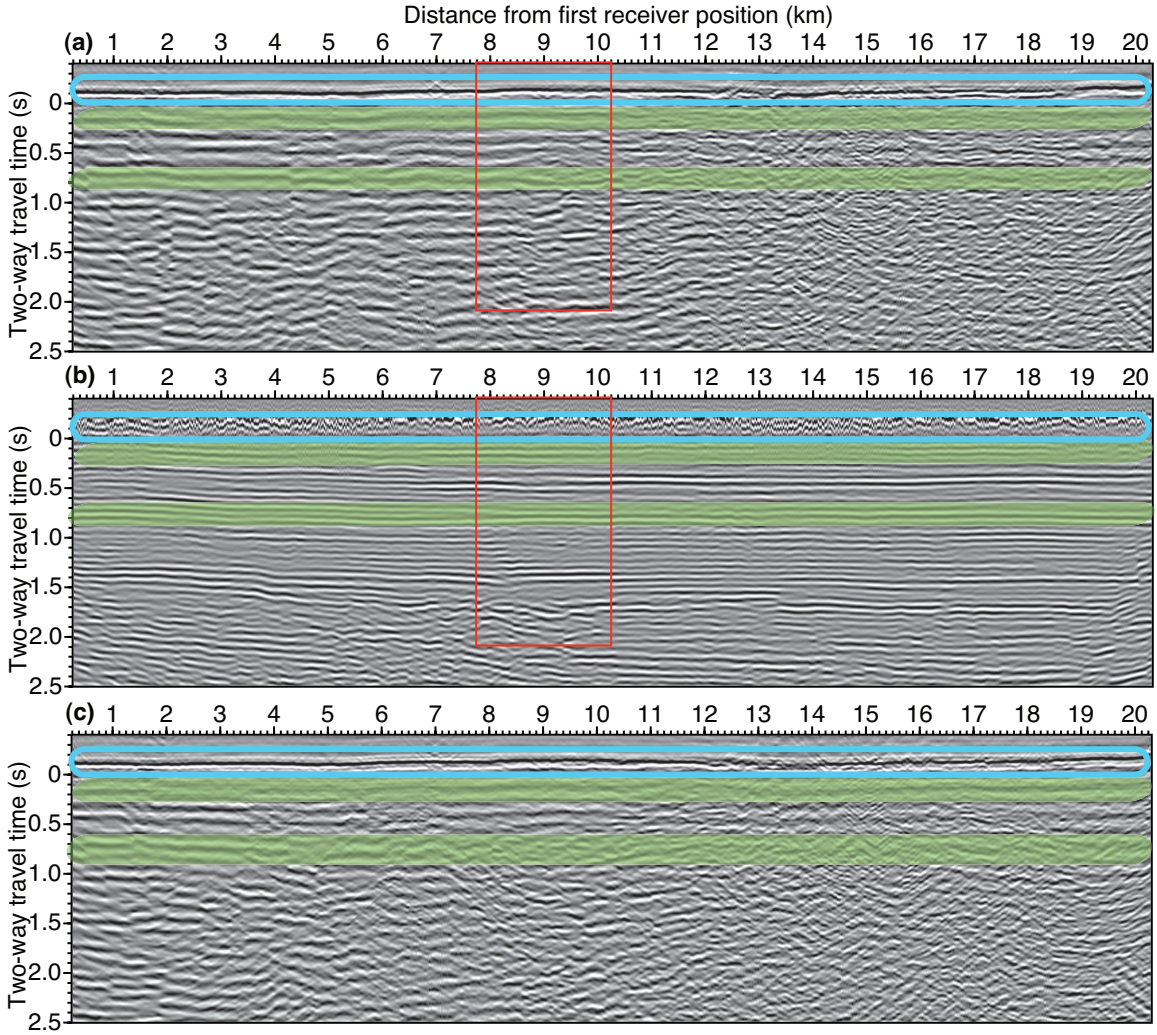

Figure 4: *Poststack time-migrated sections obtained from **(a)** the retrieved shot gathers using the velocities picked from reflections retrieved from the ambient noise, **(b)** the active data using active-data stacking velocities, and **(c)** the retrieved shot gathers using the active-data stacking velocities. Coinciding imaged reflectors are highlighted in transparent green. The blue ellipses indicate the Earth's surface. Zero-time refers to mean sea level. The red rectangles indicate the position of the section detail in Figure 5. The sections are shown after application of automatic gain control with a window of 0.5 s.*

Nevertheless, the amplitude spectra of the two results are different, which might result from the generally lower-frequency character of the retrieved shot gathers. Comparing Figure 4(a) and Figure 4(b), in particular, we observe two shallow marker events around 0.1 s and 0.8 s. These reflection events coincide in both images. In addition, there are several other coinciding coherent events. At times beyond 1 s, events in Figure 4(a) lose their spatial coherence and cannot be unambiguously identified with reflections in the active image. We also see that in the vicinity of the road the retrieved image in Figure 4(a) hardly exhibits any retrieved reflectors.

To investigate the effect of deviation of the stacking velocities picked from the retrieved virtual data with those picked from the active data on the migration image obtained from the noise, we also apply normal-moveout correction, stacking and phase-shift time migration to the virtual data using the velocities picked from the active data. This result is shown in Figure 4(c). Comparing Figure 4(c) with the result in Figure 4(a), we see that the continuity of the first event has improved, even in the vicinity of the traffic road. Furthermore, we can conclude that the apparent jump at around 3 km in Figure 4(a) may be caused by the incorrect velocity picking as it is absent in Figure 4(c). On the other hand, we see that in Figure 4(c) the spatial continuity of the deeper events has become worse. In general, we observe that the deeper the possible retrieved events, the worse the quality of their retrieval. This may be explained by the fact that the reflections are weaker and hence are drowned out by the remnants of the road-induced surface-wave noise.

Frequency analysis of the passive data reveals that these remnants are most energetic below 5 Hz. The bulk of this energy propagates as surface waves, and is removed by our processing. But even after the removal of these low frequencies, the passive data apears to have a lower frequency content than the active data. This makes the interpretation of the similarities between the active and passive data difficult. In Figure 4, we bandpass filtered both passive and active data so they have a

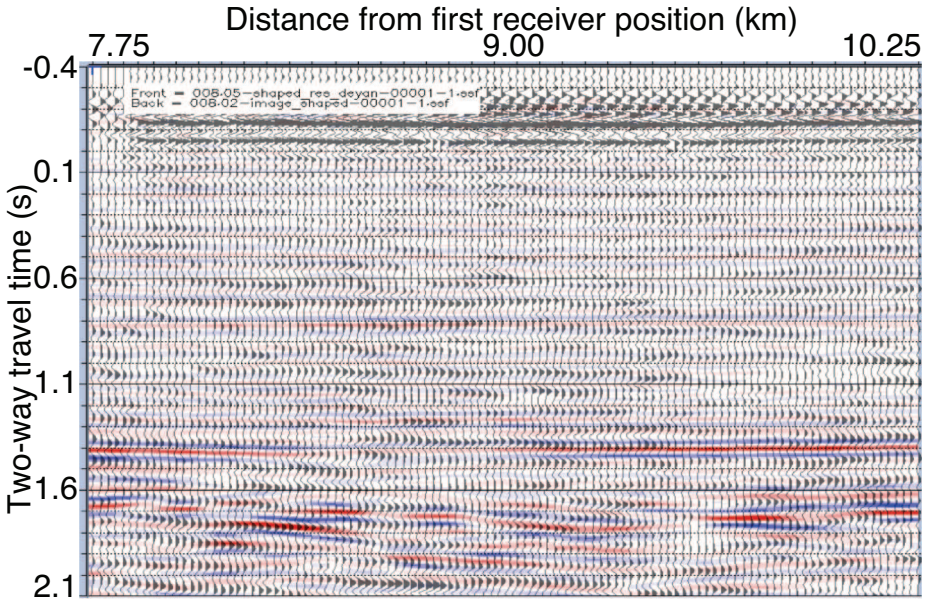

Figure 5: *Overlay of the time-migrated stacked sections in Figure 4(a) and (b) between 7.75 km and 10.25 km after application of wavelet shaping. The section from the active data is in colour, while the section from the ambient-noise data is in black.*

common frequency band, between approximately 8 and 18 Hz. Still, the lower end of this frequency band in the passive data is relatively more energetic than in the active data. In order to make a better comparison we defined a common wavelet and derived shaping filters for each data set (see Figure 6). In this way, the two data sets have the same frequency content. In addition, we applied a different gain function to the image from the retrieved data, to better match the active image. Figure 5 shows an overlay plot of a part of the two shaped images. The image of the active data is the background image (in color), while the image of the passive data is shown in black. The correspondence between the two sections is encouraging.

CONCLUSIONS

Seismic interferometry was applied to approximately 11 hours of ambient seismic noise recorded along eight lines in the north-eastern part of the Sirte Basin, East of Ajdabeya, Libya, with the aim to retrieve P-wave reflections. The crosscorrelation of noise traces resulted in retrieved virtual common-shot gathers. We processed the virtual gathers using a standard seismic processing flow. We extracted stacking velocities from the virtual data and used these to obtain poststack time-migrated reflection images. The stacking velocities were generally lower than velocities picked from an active survey along the same lines. For two-way travel times up to 3 s $\sim$ 3.5 s and for receiver positions at least several kilometers away from a traffic road bisecting the lines in their northern part, the stacking velocities from the virtual data come close to the velocities from the active data. This resulted in a good agreement between imaged reflectors in the time-migrated reflection section obtained from the ambient noise and the active-data time-migrated reflection section for two-way travel times up to 1 s. The retrieval of velocity information and reflection images from ambient seismic noise has potential applications for seismic exploration, reservoir production monitoring and CO_2 sequestration surveillance.

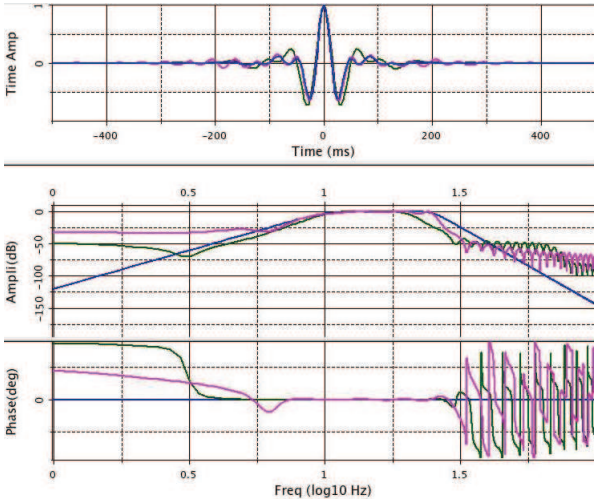

Figure 6: *Shaped wavelets as used in Figure 5 in the time domain (top) and in the frequency domain (bottom), where the blue, purple, and green colors indicate the desired, the retrieved-data, and the active-data wavelet, respectively (the later two after wavelet shaping).*

ACKNOWLEDGMENTS

The research of D.D. is sponsored by the Technology Foundation STW, applied science division of NWO (project 08115), and by Shell International Exploration & Production B.V. We thank the Libyan National Oil Company for permission to publish these results and Shell in Lybia (in particular Erik Kleiss, Rian de Jong, Mark Peach and Alan Smith) for collecting and making available the passive data.

EDITED REFERENCES

Note: This reference list is a copy-edited version of the reference list submitted by the author. Reference lists for the 2009 SEG Technical Program Expanded Abstracts have been copy edited so that references provided with the online metadata for each paper will achieve a high degree of linking to cited sources that appear on the Web.

REFERENCES

Aki, K., 1957, Space and time spectra of stationary stochastic waves, with special reference to microtremors: Bulletin of the Earthquake Research Institute, **35**, 415–457.

Campillo, M., and A. Paul, 2003, Long-range correlations in the diffuse seismic coda: Science, **299**, 547–549.

Claerbout, J. F., 1968, Synthesis of a layered medium from its acoustic transmission response: Geophysics, **33**, 264–269.

Draganov, D., X. Campman, J. Thorbecke, A. Verdel, and K. Wapenaar, 2009, Subsurface structure from ambient seismic noise: 71st Conference and Exhibition, EAGE, Extended Abstracts, Z038.

Okada, H., ed., 2003, The microtremor survey method, Geophysical Monograph Series vol.12: SEG.

Shapiro, N. M., M. Campillo, L. Stehly, and M. H. Ritzwoller, 2005, High-resolution surface wave tomography from ambient seismic noise: Science, **307**, 1615–1618.

Wapenaar, K., J. Thorbecke, D. Draganov, and J. Fokkema, 2002, Theory of acoustic daylight imaging revisited: 72nd Annual International Meeting, SEG, Expanded abstracts, 2269–2272.

Wapenaar, K., 2004, Retrieving the electrodynamic Green's function of an arbitrary inhomogeneous medium by cross-correlation: Physical Review Letters, **93**, 254301.

Yilmaz, O., 1999, Seismic data processing: SEG.